Kalman Filter Residual-Based Integrity Monitoring Against Measurement Faults

Mathieu Joerger[1] and Boris Pervan[2]
Illinois Institute of Technology, Chicago, Illinois, 60616

This paper introduces a new Kalman filter-based method for detecting sensor faults in linear dynamic systems. In contrast with existing sequential fault-detection algorithms, the proposed method enables direct evaluation of the integrity risk, which is the probability that an undetected fault causes state estimate errors to exceed predefined bounds of acceptability. The new method is also computationally efficient and straightforward to implement. The algorithm's detection test statistic is established in three steps. First, the weighted norms of current and past-time Kalman filter residuals are defined as generalized non-centrally chi-square distributed random variables. Second, these residuals are proved to be stochastically independent from the state estimate error. Third, current-time and past-time residuals are shown to be mutually independent, so that the Kalman filter-based test statistic can be recursively updated in real time by simply adding the current-time residual contribution to a previously computed weighted norm of past-time residuals. The Kalman filter-based integrity monitor is evaluated against worst-case fault profiles, which are also derived in this paper. Finally, performance analyses results are presented for an example application of aircraft precision approach navigation, where differential ranging signals from a multi-constellation satellite navigation system are filtered for positioning and carrier phase cycle ambiguity estimation.

I. Introduction

DYNAMIC estimators designed to operate under nominal conditions are vulnerable to rarely-occurring faults such as sensor failures. Detection algorithms can be implemented to mitigate the impact of sensor faults on estimator performance,[1,2] which is essential in safety-critical applications such as vehicle automation for ground and air transportation.[3,4] Of primary concern in these types of applications is the system's ability to evaluate the integrity risk, which is the probability of undetected faults causing unacceptably large estimation errors. Most approaches currently implemented in real-time systems use simple measurement processing schemes, which facilitate integrity risk monitoring at the cost of decreased estimation performance. For example, existing satellite-based navigation systems designed for aviation applications are based on snapshot position estimation,[4-6] which can limit the accuracy and fault-free integrity performance. In this paper, we derive, analyze, and evaluate a new sequential fault-detection algorithm, which opens the possibility of optimal estimation using a Kalman filter under nominal conditions, while enabling accurate and efficient integrity risk evaluation in the presence of measurement faults.

Despite multiple prior approaches (reviewed below), there is currently no widely used sequential fault-detection algorithm in safety-critical applications. One major shortcoming of published methods is their limited ability to accurately quantify integrity risk. In practice, integrity risk evaluation is needed when designing dynamic systems to achieve required levels of integrity, and it is needed operationally to predict if a mission can be safely initiated. Evaluating integrity risk includes both assessing the fault detection capability and quantifying the impact of undetected faults on state estimate errors.

Model-based fault detection methods include integrity monitoring (IM) algorithms, which provide the means for rigorous integrity risk computation. Most existing implementations of IM are 'snapshot' detection schemes.[4-6] For instance, the receiver autonomous integrity monitoring (RAIM) method used in Global Navigation Satellite Systems (GNSS) exploits redundant observations at one time of interest.[7-9] Snapshot IM is a natural choice for punctual state

[1] Senior Research Associate, Department of Mechanical, Materials and Aerospace Engineering, E-mail: joermat@iit.edu, Member AIAA.
[2] Professor, Department of Mechanical, Materials and Aerospace Engineering, E-mail: pervan@iit.edu, Associate Fellow AIAA.

estimation, but it is insufficient for sequential implementations that involve measurement filtering, for example using a Kalman filter.

The Kalman filter (KF) is a recursive estimator that exploits information from both the measurements and the system's dynamic model. The KF is widely implemented because it recursively generates optimal current-time state estimates, which maximizes current-time accuracy and fault-free integrity performance.

In safety-critical applications, the sequence of measurements used for estimation must be monitored against rare event faults. Sequential detection approaches have been investigated over the past 60 years.[10] The large majority of published algorithms have aimed at minimizing the time to detect abrupt changes in a random variable distribution.[11-15] The algorithms include multiple-hypotheses[16-18] and innovation-based methods,[19-22] and have been employed in a variety of applications including financial and medical surveillance applications,[23] industrial quality-control,[1,24] sonar noise cancellation,[25] and target tracking.[26] However, these procedures quantify the fault-detection capability in terms of detection delay, without regard to the fault's impact on state estimates, hence leaving integrity risk evaluation unaddressed.

Additional references are cited in Ref. 26: the extensive literature review of research efforts carried out over the past two decades demonstrates the lively and sustained interest for real-time sequential fault detection methods, especially in the context of tightly-coupled integration of the Global Positioning System (GPS) with Inertial Navigation Systems (INS). The most elaborate sequential fault-detection algorithms provide protection level equations, which are measures of the integrity risk in terms of position state-domain bounds. But these bounds are loose,[27-31] and they require computationally expensive processes. For example, the solution-separation approach to sequential implementations uses banks of KF,[32] whose number increases as the number of samples in the time-sequence increases.

In response, in this work, we derive a computationally-efficient KF-based IM method, which can be implemented in real-time, and does not require conservative assumptions for integrity risk computation.

In Section II of this paper, a batch least-squares residual-based IM algorithm is presented. This batch approach is similar to the well-established snapshot RAIM used in GPS applications, but it is generalized here, and applied to a sequence of measurements and of system dynamics over a finite window in time. Least-squares batch implementations can be implemented sequentially using a sliding-window mechanism. But they also require considerable computation and memory resources for the storage and processing of past-time measurements and state coefficients – which is why a KF-based IM approach is ultimately pursued.

Still, in this work, the batch IM approach is used to derive results that will be extended to KF-IM. For instance, given a time sequence of measurements and state dynamics, we can exploit the fact that the current-time state estimates are identical for a KF and for a batch. Also, a batch is expressed in a single measurement equation and is much easier to analyze than a KF (which iteratively processes multiple equations). Finally and most importantly, batch-IM highlights two conditions that facilitate direct integrity risk computation: first, the state estimate and detection test statistic are stochastically independent, and second, their probability distributions are known. The KF-IM test statistic is specifically designed to satisfy these two key-conditions.

Section III describes the KF-IM. In the first part of Section III, the weighted norm of the current-time KF residual is shown to be independent from the estimate error, and it is proved to follow a generalized non-central chi-square distribution, whose parameters are fully identified. Thus, the current-time KF test statistic fulfills the two key-conditions that enable integrity risk evaluation. But the KF also generates past-time residuals, which could be exploited to improve detection of faults that persist in time, and could provide early indicators of threats affecting current-time and future-time state estimates.

Therefore, in the second part of Section III, a cumulative KF-IM test statistic is established using both current and past-time residuals. First, the probability distributions of past-time residuals are defined. Second, it is proven that current-time state estimates and past-time residuals are statistically independent. Third, the random parts of current-time and past-time residuals are shown to be mutually independent. As a result, KF-IM achieves rigorous integrity risk evaluation using a test-statistic that can be recursively updated, by simply adding a current-time component to an accumulated past-time residual-based test statistic.

In addition, in Section IV, a method is developed to compute the worst-case fault-detection performance. Measurements collected during the filtering period are all vulnerable to rare-event integrity threats. In order to capture the impact of such failures over time, a set of realistic fault modes can be considered including impulses, steps, and ramps of all magnitudes and start times. But this set of canonical faults does not constitute a comprehensive description of all integrity threats. To circumvent this problem, a new concept is introduced for the batch-IM implementation with the derivation of theoretical worst-case faults, which maximize the integrity risk. Worst-case fault profiles are instrumental in evaluating bounds on the integrity risk.

Finally, in Section V, the integrity monitoring performance of both batch-IM and KF-IM is illustrated with an application to aircraft precision approach navigation. Sequences of code and carrier phase GNSS measurements are used for positioning and real-valued (floating) cycle ambiguity estimation. Batch-IM and KF-IM are evaluated against single-satellite fault profiles for different satellite geometries. System availability is quantified assuming a near-future GPS/Galileo carrier-phase based navigation system, at multiple locations over the Contiguous United States (CONUS).

II. Batch Residual-Based Integrity Monitoring

The batch least squares residual-based fault-detection algorithm (or batch-IM) was implemented in a previous paper[33] as a direct extension of the well-established snapshot RAIM method. Batch-IM is described below and will be used in Section III to derive results relevant to the KF-IM approach.

A linear dynamic system is described at any discrete time k of a time-sequence (spanning from time 1 to the current time noted q), by a measurement equation and a process equation:

$$\mathbf{z}_k = \mathbf{H}_k \mathbf{x}_k + \mathbf{v}_k + \mathbf{f}_k \tag{1}$$

$$\mathbf{x}_{k+1} = \mathbf{\Phi}_k \mathbf{x}_k + \mathbf{w}_k \tag{2}$$

where:

- k ranges from 1 to q
- $\mathbf{z}_k$ is the $n_k \times 1$ vector of measurements at time k
- $\mathbf{x}_k$ is the $m_k \times 1$ state vector
- $\mathbf{H}_k$ is the observation matrix
- $\mathbf{v}_k$ is the measurement noise vector
- $\mathbf{f}_k$ is the measurement-fault vector (to be detected)
- $\mathbf{\Phi}_k$ is the state transition matrix
- $\mathbf{w}_k$ is the process noise vector.

Vectors $\mathbf{v}_k$ and $\mathbf{w}_k$ are assumed normally distributed with zero mean and covariance matrices $\mathbf{V}_k$ and $\mathbf{W}_k$, respectively. We use the notation:

$$\mathbf{v}_k \sim \mathrm{N}(\mathbf{0}, \mathbf{V}_k)$$

$$\mathbf{w}_k \sim \mathrm{N}(\mathbf{0}, \mathbf{W}_k).$$

Vectors $\mathbf{v}_k$ and $\mathbf{w}_k$ are assumed independent.

A. General Batch Realization

A general batch realization is obtained by simply stacking all measurement and process equations in a single batch measurement equation:

$$\mathbf{z}_Q = \mathbf{H}_Q \mathbf{x}_Q + \mathbf{v}_Q + \mathbf{f}_Q \tag{3}$$

where

$$\mathbf{z}_Q = \begin{bmatrix} \mathbf{z}_1^T & \mathbf{0} & \cdots & \mathbf{0} & \mathbf{z}_k^T & \mathbf{0} & \cdots & \mathbf{z}_q^T \end{bmatrix}^T$$

$$\mathbf{H}_Q = \begin{bmatrix} \mathbf{H}_1 & \mathbf{0} & \cdots & & & & & \mathbf{0} \\ \mathbf{\Phi}_1 & -\mathbf{I} & \cdots & & & & & \vdots \\ \vdots & & & & & & & \\ \mathbf{0} & \cdots & & \mathbf{\Phi}_{k-1} & -\mathbf{I} & \mathbf{0} & \cdots & \mathbf{0} \\ \mathbf{0} & \cdots & & \mathbf{0} & \mathbf{H}_k & \mathbf{0} & \cdots & \mathbf{0} \\ \mathbf{0} & \cdots & & \mathbf{0} & \mathbf{\Phi}_k & -\mathbf{I} & \cdots & \mathbf{0} \\ \vdots & & & & & & & \\ \mathbf{0} & \cdots & & & & \cdots & \mathbf{0} & \mathbf{H}_q \end{bmatrix}$$

$$\mathbf{x}_Q = \begin{bmatrix} \mathbf{x}_1^T & \mathbf{x}_2^T & \cdots & \mathbf{x}_{k-1}^T & \mathbf{x}_k^T & \mathbf{x}_{k+1}^T & \cdots & \mathbf{x}_q^T \end{bmatrix}^T$$

$$\mathbf{v}_Q = \begin{bmatrix} \mathbf{v}_1^T & \mathbf{w}_1^T & \cdots & \mathbf{w}_{k-1}^T & \mathbf{v}_k^T & \mathbf{w}_k^T & \cdots & \mathbf{v}_q^T \end{bmatrix}^T$$

$$\mathbf{f}_Q = \begin{bmatrix} \mathbf{f}_1^T & \mathbf{0} & \cdots & \mathbf{0} & \mathbf{f}_k^T & \mathbf{0} & \cdots & \mathbf{f}_q^T \end{bmatrix}^T$$

For any time k, the capital subscript K designates the discrete times 1 to k (i.e., for the current time q, Q designates all discrete times during the time sequence). We respectively note n_Q and m_Q the total numbers of measurements and states for the entire time interval.

It is worth noticing that the covariance matrix $\mathbf{V}_Q$ of the batch measurement noise vector $\mathbf{v}_Q$ is block diagonal, with component block matrices:

$$\mathbf{V}_1, \quad \mathbf{W}_1, \quad \ldots \quad , \mathbf{W}_{k-1}, \quad \mathbf{V}_k, \quad \mathbf{W}_k, \quad \ldots \quad , \mathbf{V}_q$$

Measurement noise correlation can be incorporated by state augmentation.[34] Also, prior knowledge on state variables can be introduced by measurement augmentation (see Ref. 33 for example batch realizations), while preserving the block-diagonal structure of $\mathbf{V}_Q$ and the general batch formulation of Eq. (3).

B. Batch Measurement-Based State Estimation

The batch least-squares state estimate vector $\hat{\mathbf{x}}_{Q|Q}$ of $\mathbf{x}_Q$ with covariance matrix $\mathbf{P}_{Q|Q}$ (the subscript '$Q|Q$' indicates an estimate of all states using all measurements), is given by:

$$\hat{\mathbf{x}}_{Q|Q} = \mathbf{S}_Q \mathbf{z}_Q \tag{4}$$

$$\mathbf{P}_{Q|Q} = \left(\mathbf{H}_Q^T \mathbf{V}_Q^{-1} \mathbf{H}_Q\right)^{-1}$$

where $\mathbf{S}_Q$ is the pseudo-inverse of the observation matrix $\mathbf{H}_Q$ weighted by $\mathbf{V}_Q^{-1}$:

$$\mathbf{S}_Q = \left(\mathbf{H}_Q^T \mathbf{V}_Q^{-1} \mathbf{H}_Q\right)^{-1} \mathbf{H}_Q^T \mathbf{V}_Q^{-1} \tag{5}$$

The state estimate error $\delta\mathbf{x}_{Q|Q}$ is defined as:

$$\delta\mathbf{x}_{Q|Q} \equiv \hat{\mathbf{x}}_{Q|Q} - \mathbf{x}_Q = \mathbf{S}_Q\left(\mathbf{v}_Q + \mathbf{f}_Q\right) \tag{6}$$

Hazardous conditions are often determined based on a single current-time state $\delta x_{q|Q}$. (For the example aircraft approach application investigated in Section V, the emphasis is on the current-time vertical position coordinate.) The scalar $\delta x_{q|Q}$ can be expressed as:

$$\delta x_{q|Q} = \mathbf{T}_X^T \delta \mathbf{x}_{Q|Q} \tag{7}$$

where $\mathbf{T}_X$ is a $m_Q \times 1$ vector of state coefficients, all zeros except for a single element, corresponding to the state of interest, with a value of 1. We have:

$$\delta x_{q|Q} \sim \mathrm{N}(\mu_{q|Q}\ ,\ \mathbf{T}_X^T \mathbf{P}_{Q|Q} \mathbf{T}_X) \tag{8}$$

where the mean $\mu_{q|Q}$ is a function of the fault profile $\mathbf{f}_Q$:

$$\mu_{q|Q} = \mathbf{T}_X^T \mathbf{S}_Q \mathbf{f}_Q\,. \tag{9}$$

C. Batch Residual-Based Fault Detection

Similar to the snapshot residual-based IM approach,[35] a batch residual vector $\mathbf{r}_{Q|Q}$ is defined as:

$$\mathbf{r}_{Q|Q} \equiv \mathbf{z}_Q - \mathbf{H}_Q \hat{\mathbf{x}}_{Q|Q} \tag{10}$$

The norm of $\mathbf{r}_{Q|Q}$ weighted by $\mathbf{V}_Q^{-1}$ is the batch detection test statistic:

$$\left\|\mathbf{r}_{Q|Q}\right\|^2_{\mathbf{V}_Q^{-1}} = \mathbf{r}_{Q|Q}^T \mathbf{V}_Q^{-1} \mathbf{r}_{Q|Q} \tag{11}$$

From snapshot fault detection analysis,[35] the test statistic $\left\|\mathbf{r}_{Q|Q}\right\|^2_{\mathbf{V}_Q^{-1}}$ is known to follow a non-central chi-square distribution with $n_Q - m_Q$ degrees of freedom and non-centrality parameter $\lambda^2_{Q|Q}$ (which is a function of the fault vector $\mathbf{f}_Q$). We use the notation:

$$\left\|\mathbf{r}_{Q|Q}\right\|^2_{\mathbf{V}_Q^{-1}} \sim \chi^2_{NC}\left(n_Q - m_Q,\ \lambda^2_{Q|Q}\right) \tag{12}$$

$$\lambda^2_{Q|Q} = \mathbf{f}_Q^T \mathbf{V}_Q^{-1} (\mathbf{I} - \mathbf{H}_Q \mathbf{S}_Q) \mathbf{f}_Q \tag{13}$$

where $\mathbf{I}$ is the identity matrix of appropriate dimensions.

D. Integrity Risk Evaluation for Batch-IM

Integrity risk requirements are specified in terms of an alert limit ℓ, a continuity risk requirement $P_{C,R}$, and an integrity risk requirement $P_{I,R}$.[5] We consider the following events:

- Hazardous information is said to exist if the estimate error $\delta x_{q|Q}$ exceeds ℓ.
- A fault is undetected when the test statistic $\left\|\mathbf{r}_{Q|Q}\right\|^2_{\mathbf{V}_Q^{-1}}$ is smaller than a threshold $T_{Q|Q}$.

The detection threshold $T_{Q|Q}$ is set in compliance with $P_{C,R}$ to limit the probability of false alarms under fault-free (FF) conditions.[35] $T_{Q|Q}$ is derived from the following equation:

$$P\left(\left\|\mathbf{r}_{Q|Q}\right\|^2_{\mathbf{V}_Q^{-1}} \geq T_{Q|Q} \mid FF\right) = P_{C,R} \tag{14}$$

In the presence of a fault, the integrity risk or probability of hazardous misleading information P_I is defined as a joint probability:

$$P_I = P\left(\delta x_{q|Q} > \ell,\ \left\|\mathbf{r}_{Q|Q}\right\|^2_{\mathbf{V}_Q^{-1}} < T_{Q|Q}\right) \tag{15}$$

P_I is actually a conditional probability: for simplicity of notation, the condition 'given a fault' is not explicitly expressed because it is present throughout the development. The evaluation of the integrity risk P_I is necessary to assess whether the integrity performance criterion is fulfilled, i.e., if the following equation is satisfied:

$$P_I < P_{I,R} / P_P \tag{16}$$

where P_P is the prior probability of fault occurrence, which is assumed to be known (determined for example using prior experimental data).

From snapshot residual-based fault detection analysis, the random parts of $\delta x_{q|Q}$ and $\left\|\mathbf{r}_{Q|Q}\right\|^2_{\mathbf{V}_Q^{-1}}$ have been proved to be statistically independent.[35,36] It follows from Eq. (15) that the integrity risk can be expressed as a product of probabilities:

$$P_I = P\left(\delta x_{q|Q} > \ell\right) P\left(\left\|\mathbf{r}_{Q|Q}\right\|^2_{\mathbf{V}_Q^{-1}} < T_{Q|Q}\right) \tag{17}$$

In addition, the probability distributions of $\delta x_{q|Q}$ and $\left\|\mathbf{r}_{Q|Q}\right\|^2_{\mathbf{V}_Q^{-1}}$ are fully defined in Eq. (8) and (12). Therefore, the integrity risk of batch-IM can be computed.

This derivation shows that the two conditions:

- independence between state estimate error and detection test statistic
- knowledge of their probability distributions

are instrumental when evaluating the integrity risk. In Section III, a KF-based test statistic is specifically defined to satisfy these two key-conditions. But before tackling the KF-IM algorithm, a transitional step is provided by breaking down the batch residual into current and past-time components.

E. Partitioning the Batch: Equivalent Forward-Backward Smoother Formulation

We consider a fault-detection method based on a forward-backward smoother (FBS), which is equivalent to a batch, but is computationally more efficient (see Ref. 37 for additional details).

The batch residual is partitioned into individual residual components at each sample time, for the measurement and for the process equations. Each individual component can be expressed by substituting the definitions of $\mathbf{z}_Q$, $\hat{\mathbf{x}}_{Q|Q}$ and the sparse batch observation matrix $\mathbf{H}_Q$ in Eq. (3) into the residual definition of Eq. (10):

$$\mathbf{r}_{Q|Q} = \begin{bmatrix} \mathbf{r}_{1|Q} \\ \mathbf{r}_{W,1|Q} \\ \vdots \\ \mathbf{r}_{k|Q} \\ \mathbf{r}_{W,k|Q} \\ \vdots \\ \mathbf{r}_{q|Q} \end{bmatrix} = \begin{bmatrix} \mathbf{z}_1 - \mathbf{H}_1 \hat{\mathbf{x}}_{1|Q} \\ -\mathbf{\Phi}_1 \hat{\mathbf{x}}_{1|Q} + \hat{\mathbf{x}}_{2|Q} \\ \vdots \\ \mathbf{z}_k - \mathbf{H}_k \hat{\mathbf{x}}_{k|Q} \\ -\mathbf{\Phi}_k \hat{\mathbf{x}}_{k|Q} + \hat{\mathbf{x}}_{k+1|Q} \\ \vdots \\ \mathbf{z}_q - \mathbf{H}_q \hat{\mathbf{x}}_{q|Q} \end{bmatrix} \tag{18}$$

It turns out that individual residual components have simple expressions. For example, the current-time residual component $\mathbf{r}_{q|Q}$ is expressed in terms of the current-time measurement vector $\mathbf{z}_q$, the observation matrix $\mathbf{H}_q$ and of the state estimate vector $\hat{\mathbf{x}}_{q|Q}$. It can be computed at the qth forward filter iteration of the FBS (i.e., at the current-time iteration of the Kalman filter). Also, when smoothing the data backward, state estimates $\hat{\mathbf{x}}_{k|Q}$ are obtained at each preceding sampling time, so that all residual components $\mathbf{r}_{k|Q}$ and $\mathbf{r}_{W,k|Q}$ in $\mathbf{r}_{Q|Q}$ can be recovered.

In addition, we emphasized the fact that the batch measurement noise covariance matrix $\mathbf{V}_Q$ was block-diagonal. It follows that the weighted norm squared of the batch residual in Eq. (11) can be expressed as:

$$\left\|\mathbf{r}_{Q|Q}\right\|^2_{\mathbf{V}_Q^{-1}} = \sum_{k=1}^{q}\left\|\mathbf{r}_{k|Q}\right\|^2_{\mathbf{V}_k^{-1}} + \sum_{k=1}^{q-1}\left\|\mathbf{r}_{W,k|Q}\right\|^2_{\mathbf{W}_k^{-1}} \tag{19}$$

Each term of the sum corresponds to an individual residual component expressed in Eq. (18), and it is weighted by it corresponding block matrix in $\mathbf{V}_Q^{-1}$.

Particularly relevant in this work is the fact that the current-time batch residual component $\mathbf{r}_{q|Q}$ and its weighted norm can be computed using a KF. We use this observation as a starting point to derive the KF-based IM method.

III. Kalman Filter-Based Integrity Monitoring

A. Current-Time KF Test Statistic

The current-time state estimate vector $\hat{\mathbf{x}}_{q|Q}$ and residual component $\mathbf{r}_{q|Q}$ are obtained using the entire time-history of measurements, and therefore are identical for the batch and for the KF. However, this is not the case at past-time epochs, where the KF state estimate vector $\hat{\mathbf{x}}_{k|K}$ differs from the batch estimate $\hat{\mathbf{x}}_{k|Q}$. Therefore, we first consider the weighted norm of $\mathbf{r}_{q|Q}$ as a potential detection test statistic:

$$\left\|\mathbf{r}_{q|Q}\right\|^2_{\mathbf{V}_q^{-1}} = \mathbf{r}_{q|Q}^T\mathbf{V}_q^{-1}\mathbf{r}_{q|Q} \tag{20}$$

The following paragraphs address the two key-conditions that $\left\|\mathbf{r}_{q|Q}\right\|^2_{\mathbf{V}_q^{-1}}$ should satisfy to enable integrity risk evaluation.

First, the current-time KF residual vector component $\mathbf{r}_{q|Q}$ in Eq. (18) can be extracted from the batch residual vector $\mathbf{r}_{Q|Q}$ as follows:

$$\mathbf{r}_{q|Q} = \begin{bmatrix}\mathbf{0} & \mathbf{I}\end{bmatrix}\mathbf{r}_{Q|Q} \tag{21}$$

Because $\mathbf{r}_{Q|Q}$ is known to lay in the parity space – or left null space – of $\mathbf{H}_Q$,[36] it follows from Eq. (21) that vector $\mathbf{r}_{q|Q}$ exists in a subspace of the parity space of matrix $\mathbf{H}_Q$. On the other hand, $\hat{\mathbf{x}}_{q|Q}$ is derived from components of $\mathbf{z}_Q$ that belong to the range of $\mathbf{H}_Q$,[36] i.e., to the column space of $\mathbf{H}_Q$, which is the orthogonal complement of its left null space. Therefore, $\mathbf{r}_{q|Q}$ is statistically independent from $\hat{\mathbf{x}}_{q|Q}$, so that the integrity risk can be expressed as a product of probabilities:

$$P_I = P\left(\delta x_{q|Q} > \ell\right)P\left(\left\|\mathbf{r}_{q|Q}\right\|^2_{\mathbf{V}_q^{-1}} < T_{q|Q}\right) \tag{22}$$

It can be noted that KF innovation-based test statistics are not pursued in this work because, unlike the residual $\mathbf{r}_{q|Q}$ in Eq. (18), the KF innovation ($\mathbf{z}_q - \mathbf{H}_q\hat{\mathbf{x}}_{q|Q-1}$) is not independent from $\hat{\mathbf{x}}_{q|Q}$.

Second, the probability distribution of $\delta x_{q|Q}$ is given in Eq. (8). It is independent of the test statistic, and does not need to be addressed further in the remainder of the paper. However, the probability distribution of $\left\|\mathbf{r}_{q|Q}\right\|^2_{\mathbf{V}_q^{-1}}$ is as yet unknown. It is important to note that while the distribution of the total sum of partial test statistics in Eq. (19) is fully defined (by Eq. (12)), the distribution of individual terms of the sum is nevertheless undetermined.

1. Theorem I: Probability Distribution of the Current-Time Test Statistic

The current-time test statistic follows a *generalized non-central chi-square* distribution because it can be expressed as a weighted sum of independent non-central chi-square distributed random variables (proof in Section A of the Appendix):

$$\left\|\mathbf{r}_{q|Q}\right\|^2_{\mathbf{V}_q^{-1}} = \sum_{i=1}^{p_{A,q}} \alpha^2_{A,i,q} y^2_{A,i,q} \tag{23}$$

where the weights $\alpha_{A,i,q}$ (subscript i ranging from 1 to $p_{A,q}$ at current time q) and the independent random variables $y_{A,i,q}$ can be determined by singular value decomposition (SVD) of matrix $\mathbf{A}$:

$$\mathbf{A} = \mathbf{V}_q^{-1/2}\begin{bmatrix}\mathbf{0} & \mathbf{I}\end{bmatrix}\left(\mathbf{I} - \mathbf{H}_Q\mathbf{S}_Q\right)\mathbf{V}_Q^{1/2} \tag{24}$$

The SVD is noted: $\mathbf{A} = \mathbf{U}_{LA}\mathbf{\Lambda}_A\mathbf{U}_{RA}^T$.

The coefficient $\alpha_{A,i,q}$ is the ith non-zero element of the diagonal matrix $\mathbf{\Lambda}_A$ and

$$y_{A,i,q} \sim \mathrm{N}\left(\mathbf{T}_A^T\mathbf{U}_{RA}^T\mathbf{V}_Q^{-1/2}\mathbf{f}_Q\ ,\ 1\right)$$

where the matrix $\mathbf{T}_A^T = \begin{bmatrix}\mathbf{0} & 1 & \mathbf{0}\end{bmatrix}$ is used to extract the ith row of $\mathbf{U}_{RA}^T$.

Equation (23) defines a generalized non-central chi-square distribution. It cannot be expressed analytically without an integral form or an infinite sum,[38] but its cumulative distribution function (CDF) can be computed numerically to any desired level of accuracy using published algorithms (we use Ref. 39).

However, Theorem I expresses the probability distribution of a partial test-statistic in terms of batch matrices (subscripts Q in Eq. (24)). In practice, processing batch matrices is computationally and memory expensive, so a recursive version is defined below.

Consider the current-time KF measurement update equation:

$$\hat{\mathbf{x}}_{q|Q} = \mathbf{K}_q\mathbf{z}_q + \left(\mathbf{I} - \mathbf{K}_q\mathbf{H}_q\right)\hat{\mathbf{x}}_{q|Q-1} \tag{25}$$

where $\mathbf{K}_q$ is the current-time KF gain. The right-hand-side terms in Eq. (25) were arranged to isolate two statistically independent random vectors $\mathbf{z}_q$ and $\hat{\mathbf{x}}_{q|Q-1}$. Also, Eq. (18) established that:

$$\mathbf{r}_{q|Q} = \mathbf{z}_q - \mathbf{H}_q\hat{\mathbf{x}}_{q|Q} \tag{26}$$

Substituting Eq. (25) into (26) results in:

$$\mathbf{r}_{q|Q} = \left(\mathbf{I} - \mathbf{H}_q\mathbf{K}_q\right)\mathbf{z}_q - \mathbf{H}_q\left(\mathbf{I} - \mathbf{K}_q\mathbf{H}_q\right)\hat{\mathbf{x}}_{q|Q-1} \tag{27}$$

This current-time residual component is normally distributed with covariance matrix

$$\mathbf{R}_{q|Q} = \left(\mathbf{I} - \mathbf{H}_q \mathbf{K}_q\right)\mathbf{V}_q \left(\mathbf{I} - \mathbf{H}_q \mathbf{K}_q\right)^T - \mathbf{H}_q \left(\mathbf{I} - \mathbf{K}_q \mathbf{H}_q\right)\mathbf{P}_{q|Q-1} \left(\mathbf{I} - \mathbf{K}_q \mathbf{H}_q\right)^T \mathbf{H}_q^T \tag{28}$$

where $\mathbf{P}_{q|Q-1}$ is the state prediction covariance matrix of $\hat{\mathbf{x}}_{q|Q-1}$.

2. *Corollary to Theorem I: Distribution of the Current-Time Test Statistic for Recursive Implementation*
The current-time test statistic can be expressed as:

$$\left\|\mathbf{r}_{q|Q}\right\|^2_{\mathbf{V}_q^{-1}} = \sum_{i=1}^{p_q} \alpha_{i,q}^2 y_{i,q}^2 \tag{29}$$

where $\alpha_{i,q}$ are the p_q non-zero singular values of $\mathbf{B}$,

$$\mathbf{B} = \mathbf{V}_q^{-1/2} \mathbf{R}_{q|Q}^{1/2} = \mathbf{U}_L \mathbf{\Lambda} \mathbf{U}_R^T \tag{30}$$

and

$$y_{i,q} \sim \mathrm{N}\left(\begin{bmatrix}\mathbf{0} & \alpha_{i,q}^{-1} & \mathbf{0}\end{bmatrix}\mathbf{U}_L^T \mathbf{V}_q^{-1/2}\left(\mathbf{f}_q - \mathbf{H}_q \boldsymbol{\mu}_{q|Q}\right),\ 1\right)$$

where $\mathbf{f}_q$ is the current-time vector component of $\mathbf{f}_Q$ and $\boldsymbol{\mu}_{q|Q}$ is the mean of $\hat{\mathbf{x}}_{q|Q}$. A complete proof of this corollary is presented in Section B of the Appendix (the proof is complicated by the fact that, in general, $\mathbf{R}_{q|Q}$ is not full-rank).

At this point, we have shown that the weighted norm of the current-time KF residual in Eq. (20) enables direct integrity risk evaluation because it is independent of the current-time state estimate error, and because its probability distribution is fully defined. The next paragraphs will show that past-time KF residuals can also be exploited. Past-time residuals can improve the detection of faults that persist in time, and provide early indicators of faults affecting current-time state estimates.

B. Cumulative KF Test Statistic

The method described in this section shows how past-time KF residuals $\mathbf{r}_{k|K}$ can be used to compute a cumulative KF-IM test statistic. Unlike current-time state estimates and residual vector components, past-time components for the KF ($\hat{\mathbf{x}}_{k|K}$ and $\mathbf{r}_{k|K}$) differ from the batch components ($\hat{\mathbf{x}}_{k|Q}$ and $\mathbf{r}_{k|Q}$). In response, at any past-time epoch *k*, we consider a *subset* batch measurement equation, represented in Fig. 1 as a partition of the full batch (introduced in Eq. 3). The subset batch measurement equation is expressed as:

$$\mathbf{z}_K = \mathbf{H}_K \mathbf{x}_K + \mathbf{v}_K + \mathbf{f}_K \tag{31}$$

The subset batch representation facilitates the analysis of $\mathbf{r}_{k|K}$. For instance, the state estimate vector $\hat{\mathbf{x}}_{k|K}$ at epoch *k* is the same for the KF as for the subset batch. And results that were established at the last epoch of the full batch are valid at the last epoch of the subset batch. In particular, the partial residual component at epoch *k* is the same for the KF and for the subset batch, and is given by:

$$\mathbf{r}_{k|K} = \mathbf{z}_k - \mathbf{H}_k \hat{\mathbf{x}}_{k|K} \tag{32}$$

The weighted norm of the residual in Eq. (32) is written as:

$$\left\|\mathbf{r}_{k|K}\right\|^2_{\mathbf{V}_k^{-1}} = \mathbf{r}_{k|K}^T \mathbf{V}_k^{-1} \mathbf{r}_{k|K} \tag{33}$$

which can easily be computed at epoch *k* using a KF.

$$
\begin{bmatrix} \mathbf{z}_1 \\ \mathbf{0} \\ \vdots \\ \mathbf{0} \\ \mathbf{z}_k \\ \mathbf{0} \\ \vdots \\ \mathbf{z}_q \end{bmatrix}
=
\begin{bmatrix}
\mathbf{H}_1 & \mathbf{0} & \cdots & & & & & \mathbf{0} \\
\mathbf{\Phi}_1 & -\mathbf{I} & \cdots & & & & & \vdots \\
\vdots & & & & & & & \\
\mathbf{0} & \cdots & & \mathbf{\Phi}_{k-1} & -\mathbf{I} & \mathbf{0} & \cdots & \mathbf{0} \\
\mathbf{0} & \cdots & & \mathbf{0} & \mathbf{H}_k & \mathbf{0} & \cdots & \mathbf{0} \\
\mathbf{0} & \cdots & & \mathbf{0} & \mathbf{\Phi}_k & -\mathbf{I} & \cdots & \mathbf{0} \\
\vdots & & & & & & & \\
\mathbf{0} & \cdots & & & & \cdots & \mathbf{0} & \mathbf{H}_q
\end{bmatrix}
\begin{bmatrix} \mathbf{x}_1 \\ \mathbf{x}_2 \\ \vdots \\ \mathbf{x}_{k-1} \\ \mathbf{x}_k \\ \mathbf{x}_{k+1} \\ \vdots \\ \mathbf{x}_q \end{bmatrix}
+
\begin{bmatrix} \mathbf{v}_1 \\ \mathbf{w}_1 \\ \vdots \\ \mathbf{w}_{k-1} \\ \mathbf{v}_k \\ \mathbf{w}_k \\ \vdots \\ \mathbf{v}_q \end{bmatrix}
+
\begin{bmatrix} \mathbf{f}_1 \\ \mathbf{0} \\ \vdots \\ \mathbf{0} \\ \mathbf{f}_k \\ \mathbf{0} \\ \vdots \\ \mathbf{f}_q \end{bmatrix}
$$

Fig. 1 Full Batch and Subset Batch Realizations

One can briefly note that the full batch residual vector in Eq. (18) included contributions $\mathbf{r}_{W,k|Q}$ from the state transition model. In contrast, residual components corresponding to KF state predictions are null:

$$\mathbf{r}_{W,k|K} = -\mathbf{\Phi}_k \hat{\mathbf{x}}_{k|K} + \hat{\mathbf{x}}_{k+1|K} = \mathbf{0} \tag{34}$$

This means that the KF-IM residual is ineffective in detecting plant and actuator faults. In systems that are vulnerable to these types of threats, batch-IM (or FBS-IM) can be implemented instead.

The next paragraphs will show that $\left\|\mathbf{r}_{k|K}\right\|^2_{\mathbf{V}_k^{-1}}$ satisfies the two key-conditions required for accurate integrity risk evaluation.

First, the probability distribution of the partial residual's weighted norm $\left\|\mathbf{r}_{k|K}\right\|^2_{\mathbf{V}_k^{-1}}$ is determined using Theorem I and its Corollary. Theorem I can be derived for the last epoch of the subset batch instead of the full batch. Proof of the Corollary for past-time residuals is easily established using Eq. (32). Both Theorem I and its Corollary remain valid when replacing current-time subscripts q and Q with past-time indices k and K in the proofs of Sections A and B of the Appendix.

Second, independence between the current-time state estimate $\delta x_{q|Q}$ and past-time KF residuals $\mathbf{r}_{k|K}$ is established in Theorem II.

1. Theorem II: Statistical Independence between Current-Time State Estimates and Past-Time Test-Statistics

The random parts of the current-time state estimate vector $\hat{\mathbf{x}}_{q|Q}$ and of the past-time KF residual vector component $\mathbf{r}_{k|K}$, at any epoch k of the filtering interval, are derived from orthogonal components of the batch measurement noise vector $\mathbf{v}_Q$. A complete proof of this theorem is given in Section C of the Appendix, where $\hat{\mathbf{x}}_{q|Q}$ and $\mathbf{r}_{k|K}$ are expressed in terms of components of $\mathbf{v}_Q$ respectively belonging to the range space of $\mathbf{H}_Q$ and to the null space of $\mathbf{H}_Q$.

Theorem II shows that both current and past-time residual components can contribute to the KF-IM test statistic. The last step of the algorithm derivation provides a straightforward solution to combine current-time and past-time residuals.

The cumulative KF-IM test statistic $r_{KF,Q}$ is defined as a sum of weighted norms squared of current and past-time residual components:

$$r_{KF,Q} = \sum_{k=1}^{q} \left\|\mathbf{r}_{k|K}\right\|^2_{\mathbf{V}_k^{-1}} \tag{35}$$

Summing residual contributions over discrete times 1 to q aims at increasing fault detectability by exploiting the cumulative impact of a fault over time (similar to Eq. (19) for the batch implementation), rather than its instantaneous, current-time impact as in Section III-A. The test statistic $r_{KF,Q}$ is easily, recursively updated by

adding the current-time KF residual component $\left\|\mathbf{r}_{q|Q}\right\|^2_{\mathbf{V}^{-1}_{V,q}}$ to the previously computed test-statistic $r_{KF,Q-1}$. Its probability distribution is determined using Theorem III.

2. Theorem III: Mutual Independence between Current-Time and Past-Time Residuals

The random parts of current and past-time KF residual components $\mathbf{r}_{k|K}$ at all epochs k are mutually independent. The proof of Theorem III is presented in Section D of the Appendix. It is established using Theorem II in an expression of the partial residual $\mathbf{r}_{k|K}$ akin to Eq. (27).

According to Theorem III, the KF residual components $\mathbf{r}_{k|K}$ whose norms squared are summed in Eq. (35) are all mutually independent. Equation (35) can be rewritten using the Corollary to Theorem I as:

$$r_{KF,Q} = \sum_{k=1}^{q}\sum_{i=1}^{p_k}\alpha_{i,k}^2 y_{i,k}^2 \tag{36}$$

We have shown that the variables $y_{i,k}$ are all mutually independent, normally distributed random variables. It follows that $r_{KF,Q}$ in Eq. (36) is expressed as a generalized non-central chi-square distribution, whose parameters are fully identified.

The full KF-IM test statistic is shown in Theorem II to be statistically independent from the estimate error. Let T_{KF} be the KF-IM detection threshold, computed similarly to $T_{Q|Q}$ in Eq. (14). In the presence of a fault, the integrity risk of KF-IM can ultimately be evaluated as:

$$P_I = P\left(\delta x_{q|Q} > \ell\right)P\left(r_{KF,Q} < T_{KF}\right) \tag{37}$$

IV. Worst Case Fault Derivation

In order to protect the dynamic system against all potential sensor faults, the integrity risk must be conservatively evaluated. An upper bound on the integrity risk can be determined for the worst-case fault magnitude (i.e., for the norm of the fault vector that maximizes the integrity risk), and for the worst-case fault mode. The fault mode designates the subset of measurements affected by the fault, i.e., the non-zero elements of the fault vector. In sequential fault detection, which is carried out over multiple time-epochs, we not only consider the fault mode and magnitude, but also the fault profile over time.

Application-specific solutions have been implemented in the literature (e.g., Ref. 16, 31). For instance, step and ramp-type fault models of all magnitudes and start times are assumed in Ref. 40. Such basic fault profiles may account for some realistic integrity threats affecting some sensors, but they do not provide a comprehensive description of all potential faults. A more direct approach is investigated here by deriving theoretical faults specifically designed to maximize the integrity risk P_I. In this paper, we establish worst-case fault profiles for the batch IM process. For comparison purposes, the same fault profiles are used for batch-IM and KF-IM in performance evaluations of Section V. Worst-case fault profiles for KF-based method will be analyzed in future work.

The worst-case fault maximizes the batch position estimate error (most hazardous) while minimizing the residual (most misleading). Fault vectors that belong to the range space of $\mathbf{H}_Q$ (e.g., $\mathbf{f}_Q = \mathbf{H}_Q\mathbf{x}_W$, for any $n_Q \times 1$ vector $\mathbf{x}_W$) are strictly undetectable using the residual ($\lambda^2_{Q|Q}$ in Eq. (13) is zero). In this case, the impact of the vector $\mathbf{x}_W$ is entirely transferred onto the state estimate error vector $\delta\mathbf{x}_{Q|Q}$ in Eq. (6).

This observation illustrates a fundamental limitation of the residual-based fault detection method, which cannot ensure detection against faults affecting more than n_{MAX} measurements.[35] The number n_{MAX} is the difference between the number of sensor measurements and the number of unknown states (i.e., states without prior knowledge). Fortunately, if measurement sources are independent, the probability of occurrence of multiple simultaneous sensor failures is often extremely low. In this work, we assume that multiple simultaneous sensor failures do not cause the number of faulted measurements to exceed n_{MAX}. A method to account for the integrity risk caused by the unlikely event of a number of failed measurements higher than n_{MAX} is provided in Ref. 40.

A fault on a subset of sensors affects a subset of elements of the fault vector $\mathbf{f}_Q$. Let n_{NZ} be the number of non-zero elements in $\mathbf{f}_Q$ (i.e., the number of faulty samples). As discussed in the previous paragraph, n_{NZ} shall not exceed n_{MAX}. The vector $\mathbf{f}_Q$ may be expressed as:

$$\mathbf{f}_Q = \mathbf{T}_Z \mathbf{f}_{NZ} . \tag{38}$$

where $\mathbf{T}_Z$ is a $n_Q \times n_{NZ}$ sparse matrix of zeroes and ones that extracts the non-zero elements of $\mathbf{f}_Q$, and $\mathbf{f}_{NZ}$ is the $n_{NZ} \times 1$ vector containing these non-zero elements. Each column of $\mathbf{T}_Z$ has a single non-zero element: a unity coefficient at the ith row and j^{th} column of $\mathbf{T}_Z$ attributes the jth element of $\mathbf{f}_{NZ}$ to the ith measurement-fault in $\mathbf{f}_Q$.

Equations (9) and (13) indicate that the fault vector $\mathbf{f}_Q$ affects the mean $\mu_{q|Q}$ of $\delta x_{q|Q}$ and the non-centrality parameter $\lambda^2_{Q|Q}$ of the residual $\mathbf{r}_{Q|Q}$. The ratio $\mu^2_{q|Q} / \lambda^2_{Q|Q}$ is named the failure mode slope g_{FM}, and is expressed as:

$$g^2_{FM} = \frac{\mathbf{f}^T_{NZ} \mathbf{T}^T_Z \mathbf{S}^T_Q \mathbf{T}^T_X \mathbf{T}_X \mathbf{S}_Q \mathbf{T}_Z \mathbf{f}_{NZ}}{\mathbf{f}^T_{NZ} \mathbf{T}^T_Z \mathbf{V}^{-1}_Q \left(\mathbf{I} - \mathbf{H}_Q \mathbf{S}_Q\right) \mathbf{T}_Z \mathbf{f}_{NZ}} , \tag{39}$$

In order to determine the direction of vector $\mathbf{f}_{NZ}$ that maximizes g_{FM}, a change of variable is performed by defining $\mathbf{f}_{NZ*}$ as

$$\mathbf{f}_{NZ*} \equiv \left(\mathbf{T}^T_Z \mathbf{V}^{-1}_Q \left(\mathbf{I} - \mathbf{H}_Q \mathbf{S}_Q\right) \mathbf{T}_Z\right)^{1/2} \mathbf{f}_{NZ} . \tag{40}$$

The following definition is used in the next steps of the derivation:

$$\mathbf{M}^{-1}_Z = \left(\mathbf{T}^T_Z \mathbf{V}^{-1}_Q \left(\mathbf{I} - \mathbf{H}_Q \mathbf{S}_Q\right) \mathbf{T}_Z\right)^{1/2} . \tag{41}$$

The matrix $\mathbf{V}^{-1}_Q (\mathbf{I} - \mathbf{H}_Q \mathbf{S}_Q)$ is of rank $n_Q - m_Q$. The matrix $\mathbf{M}^{-1}_Z$ is $n_{NZ} \times n_{NZ}$ and is full rank for any $\mathbf{T}_Z$ corresponding to a single-sensor fault (or to a fault affecting a small subset of sensors). In this case, $\mathbf{f}_{NZ}$ is given by:

$$\mathbf{f}_{NZ} = \mathbf{M}_Z \mathbf{f}_{NZ*} , \tag{42}$$

and the failure mode slope can be rewritten as:

$$g^2_{FM} = \frac{\mathbf{f}^T_{NZ*} \mathbf{M}^T_Z \mathbf{M}^T_X \mathbf{M}_X \mathbf{M}_Z \mathbf{f}_{NZ*}}{\mathbf{f}^T_{NZ*} \mathbf{f}_{NZ*}} . \tag{43}$$

where

$$\mathbf{M}_X = \mathbf{T}_X \mathbf{S}_Q \mathbf{T}_Z . \tag{44}$$

The vector $\mathbf{f}_{NZ*}$ that maximizes g^2_{FM} is the eigenvector $\mathbf{v}_{MAX}$ corresponding to the largest eigenvalue of the symmetric matrix $\mathbf{M}^T_Z \mathbf{M}^T_X \mathbf{M}_X \mathbf{M}_Z$. A similar derivation can be found in Ref. 41 in the context of snapshot RAIM, for single-epoch faults simultaneously affecting multiple measurements. Finally, the worst-case fault $\mathbf{f}_{WORST}$ that maximizes the probability of hazardous misleading information is:

$$\mathbf{f}_{WORST} = \mathbf{T}_Z \mathbf{M}_Z \mathbf{v}_{MAX} . \tag{45}$$

V. Performance Analysis

Performance comparisons for an illustrative example of a near-future multi-constellation navigation system are carried out to quantify the integrity risk of batch-IM versus KF-IM.

A. Availability Analysis for Aircraft Precision Approach

The performance analysis is structured around an example application of precision navigation for aircraft approach and landing. During precision approach under limited visibility, the pilot makes the decision of whether to initiate or to abort the mission based on the computed integrity risk. Therefore, in this application, timely and accurate integrity risk evaluation is critical. Then, aircraft approach navigation requirements are extremely stringent.[5] They are challenging to satisfy using 'snapshot' positioning, but might be fulfilled using measurement filtering over time. The batch-IM method could be implemented, but airplanes have limited computation and memory resources. Instead, the KF-IM algorithm can enable real-time evaluation of tight bounds on the integrity risk.

In addition, in this example application, aircraft navigation is based on near-term future GNSS ranging signals from GPS and Galileo satellites. GNSS carrier phase ranging measurements are biased by cycle ambiguities, which remain constant for as long as the signal is continuously tracked. In this case, the dynamic model accounts for the constant cycle ambiguity biases. Measurement models also account for sources of time-correlated errors. These simple yet realistic measurement and process models are used to illustrate the batch-IM and KF-IM performance.

The measurement model used in this work is similar to the one described in Ref. 33. Differential GNSS measurements used for aircraft positioning include code phase (pseudorange) $\boldsymbol{\rho}_k$ and carrier phase $\boldsymbol{\varphi}_k$ signals.[42] At each measurement time k, these observations are stacked together for all satellites in a measurement vector:

$$\begin{bmatrix} \boldsymbol{\rho} \\ \boldsymbol{\varphi} \end{bmatrix}_k = \begin{bmatrix} \mathbf{G}_k & 1 & \mathbf{0} & \mathbf{H}_{ERR,\rho,k} \\ \mathbf{G}_k & 1 & \mathbf{I}_{n_k} & \mathbf{H}_{ERR,\phi,k} \end{bmatrix} \begin{bmatrix} \mathbf{x}_{U,k} \\ \tau_k \\ \mathbf{n} \\ \mathbf{s}_{ERR,k} \end{bmatrix} + \begin{bmatrix} \mathbf{v}_\rho \\ \mathbf{v}_\phi \end{bmatrix}_k \tag{46}$$

where

$\mathbf{G}_k$ is the satellite geometry matrix (made of line of sight unit vectors for all satellites in view)

$\mathbf{x}_{U,k}$ is the user position (in a local reference frame),

τ_k is the differential receiver clock bias

$\mathbf{n}$ is the vector of differenced cycle ambiguities

Differential code and carrier phase receiver noise vectors are respectively defined as:

$$\mathbf{v}_{\rho,k} \sim \mathrm{N}\left(\mathbf{0},\ \mathbf{I}\sigma_\rho^2\right) \quad \text{and} \quad \mathbf{v}_{\phi,k} \sim \mathrm{N}\left(\mathbf{0},\ \mathbf{I}\sigma_\phi^2\right) \tag{47}$$

In addition, a vector of error states $\mathbf{s}_{ERR}$ is appended to the estimated states to incorporate the dynamics of the error sources described below. The matrix $\mathbf{H}_{ERR}$ contains the corresponding state coefficients.

The process equation accounts for various types of dynamics. It is expressed as:

$$\begin{bmatrix} \mathbf{x}_{U,k+1} \\ \tau_{k+1} \\ \mathbf{n} \\ \mathbf{s}_{ERR,k+1} \end{bmatrix} = \begin{bmatrix} \mathbf{0} & \mathbf{0} & \mathbf{0} & \mathbf{0} \\ \mathbf{0} & 0 & \ddots & \vdots \\ \vdots & \ddots & \mathbf{I} & \mathbf{0} \\ \mathbf{0} & \cdots & \mathbf{0} & \boldsymbol{\Phi}_{ERR,k} \end{bmatrix} \begin{bmatrix} \mathbf{x}_{U,k} \\ \tau_k \\ \mathbf{n} \\ \mathbf{s}_{ERR,k} \end{bmatrix} + \begin{bmatrix} \mathbf{w}_U \\ \mathbf{w}_T \\ \mathbf{0} \\ \mathbf{w}_{ERR} \end{bmatrix}_k \tag{48}$$

Equation (48) includes states whose time propagation is unknown ($\mathbf{x}_{U,k}$ and τ_k) and for which the zero-mean normally-distributed process noise ($\mathbf{w}_U$ and $\mathbf{w}_T$) has a very large standard deviation. The cycle ambiguity vector $\mathbf{n}$ is initially unknown, but is constant over time (the corresponding process noise vector component is $\mathbf{0}$). The vector $\mathbf{w}_{ERR}$ is the process noise on error states $\mathbf{s}_{ERR}$.

The satellite ranging error models (captured in $\mathbf{H}_{ERR}$, $\mathbf{\Phi}_{ERR}$, $\mathbf{s}_{ERR}$, and $\mathbf{w}_{ERR}$) are described in detail in Ref. 33. They are not essential for the performance analysis, but they were included to demonstrate that KF-IM can be efficiently implemented in a realistic dynamic system. Thus, satellite orbit ephemeris errors are modeled as ramps over time with constant gradients. Vertical tropospheric decorrelation is modeled as an exponential function of the change in aircraft altitude multiplied by a constant tropospheric refractivity index.[43] The unknown but constant gradients and tropospheric parameter are included as states in $\mathbf{s}_{ERR}$ and assumed constant over time (corresponding elements in $\mathbf{w}_{ERR}$ are zero-valued). Ionospheric delay is eliminated using dual-frequency code and carrier measurements.[42] Time-correlated noise due to multipath signal reflections is modeled as a first order Gauss Markov Process (GMP) with a 1 min time-constant, and is also incorporated by state augmentation in $\mathbf{s}_{ERR}$ (the corresponding elements in $\mathbf{w}_{ERR}$ are the zero-mean normally-distributed driving noise vector of the multipath error's GMP).

The fault-free measurement equation (46) and process equation (48) are expressed in the form of Eqs (1) and (2). The fault vector $\mathbf{f}_k$ assumes single-satellite faults, and is derived using the worst-case fault profile expressed in Eq. (45). Equations (46), (48), and (45) are used to evaluate bounds on the integrity risk using batch-IM and KF-IM as described in Eq. (17) and (37) of Sections II and III, respectively.

In this analysis, the airplane is assumed to follow a straight-in trajectory toward the runway, at a constant 70 m/s velocity, along a constant 3 deg glideslope angle. Hazardous information is determined based on the vertical position coordinate. Navigation requirements in Eq. (14), (17) and (37) include a vertical alert limit ℓ of 10 m, a continuity risk requirement $P_{C,R}$ of $8 \cdot 10^{-6}$ and an integrity risk requirement $P_{I,R}$ of 10^{-7}. [5] The prior probability of fault P_P is derived from the single-satellite failure rate of $10^{-4}/\text{hr}$.[5] Measurements are assumed sampled at regular 20 s intervals over a 5 min mission duration. To account for different satellite geometries, approaches starting at regular 4 min intervals are considered over a 24 hour period. The percentage of approaches that meets the integrity performance criterion in Eq. (16) over the total number of simulated approaches is the measure of fault-detection performance called availability.

B. Performance Comparison between Batch-IM and KF-IM over CONUS

The performance of the batch and KF integrity monitoring methods is analyzed for a $5\text{deg} \times 5\text{deg}$ latitude-longitude grid of locations over CONUS. The same sequence of measurements and the same fault profiles are used in both algorithms.

Fig. 2 and 3 present availability maps for the batch-IM and KF-IM methods, respectively. Availability is color-coded: white color corresponds to a value of 100%, black represents 85%. Constant availability contours are also displayed. In both batch-IM and KF-IM, availability ranges between 96% and 100%. Higher availability for batch-IM is to be expected because the sensitivity of past-time batch residuals (computed using $\hat{\mathbf{x}}_{k|Q}$ in Eq. (18)) is higher than that of past-time KF residuals (derived from $\hat{\mathbf{x}}_{k|K}$). Still, for this example application, the new recursive KF-based fault-detection algorithm performs almost as well as batch-IM, which is much more computationally and memory intensive.

Fig. 4 displays the availability map of a KF-IM approach that only uses the norm of the current-time residual as test statistic (as derived in Section III-A). The color code was modified in Fig.4 where black corresponds to 45%, white to 100%. Availability drops below 50% at a few locations, versus 96% for the full KF-IM method. Fig. 4 emphasizes the benefit of using both current and past-time KF residuals.

VI. Conclusion

This paper introduced a new Kalman filter-based sensor fault detection method for dynamic systems that require measurement filtering over time. A recursively-updated KF-IM test statistic was designed to exploit both current-time and past-time residual contributions while satisfying two key-conditions. First, the test statistic was proved to be stochastically independent from the current-time state estimate error. Second, it was shown to follow a generalized non-central chi-square distribution. As a result, this easy-to-implement KF-IM algorithm enables direct and rigorous integrity risk evaluation. Availability analyses were carried out for an example aircraft navigation application where differential GNSS carrier phase signals were used for positioning. Results showed that the new recursive method could achieve a level of performance similar to that of a much more computationally and memory-expensive batch fault-detection process. KF-IM opens the possibility for efficient, real-time KF-based estimation with the assurance of a tight bound on the integrity risk.

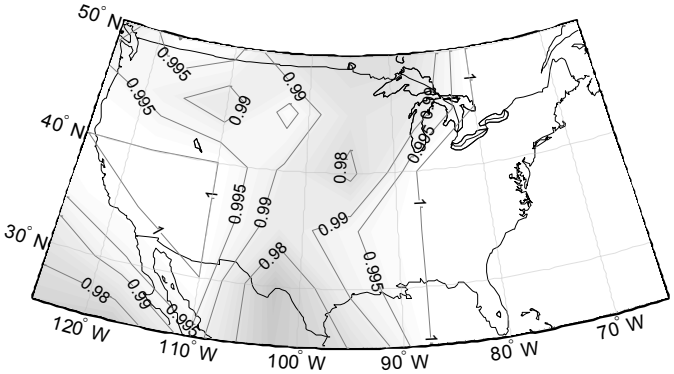

Fig. 2 Availability Map for Batch-IM

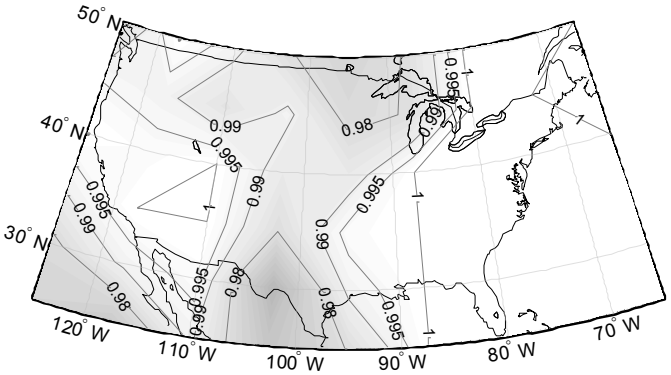

Fig. 3 Availability Map for KF-IM

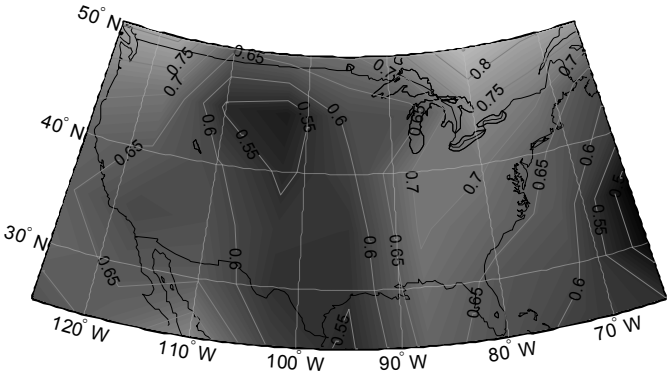

Fig. 4 Availability Map Using Only the Current-Time KF-IM Residual

Appendix

A. Proof of Theorem I: Probability Distribution of the Current-Time Test Statistic

The current-time component of the batch residual vector can be expressed using the definitions of Eq. (4), (10), and (18) as:

$$\mathbf{r}_{q|Q} = \begin{bmatrix}\mathbf{0} & \mathbf{I}\end{bmatrix}\left(\mathbf{I} - \mathbf{H}_Q\mathbf{S}_Q\right)\mathbf{z}_Q . \tag{49}$$

The first step of the proof is to normalize the measurement vector $\mathbf{z}_Q$. Consider the change of variable

$$\mathbf{z}_{Q*} = \mathbf{V}_Q^{-1/2}\mathbf{z}_Q \quad , \quad \mathbf{z}_{Q*} \sim \mathrm{N}\left(\mathbf{V}_Q^{-1/2}\mathbf{f}_Q \ , \ \mathbf{I}\right) \tag{50}$$

The vector $\mathbf{z}_{Q*}$ of independent, identically distributed (i.i.d.) random variables is substituted back into Eq. (35):

$$\mathbf{r}_{q|Q} = \begin{bmatrix}\mathbf{0} & \mathbf{I}\end{bmatrix}\left(\mathbf{I} - \mathbf{H}_Q\mathbf{S}_Q\right)\mathbf{V}_Q^{1/2}\mathbf{z}_{Q*} . \tag{51}$$

The weighted norm of $\mathbf{r}_{q|Q}$ defined in Eq. (20) can be expressed as a quadratic form of i.i.d. Gaussian random variables:

$$\left\|\mathbf{r}_{q|Q}\right\|^2_{\mathbf{V}_q^{-1}} = \mathbf{z}_{Q*}^T\mathbf{A}^T\mathbf{A}\mathbf{z}_{Q*} \tag{52}$$

where

$$\mathbf{A} = \mathbf{V}_q^{-1/2}\begin{bmatrix}\mathbf{0} & \mathbf{I}\end{bmatrix}\left(\mathbf{I} - \mathbf{H}_Q\mathbf{S}_Q\right)\mathbf{V}_Q^{1/2} \tag{53}$$

The singular value decomposition (SVD) of $\mathbf{A}$ is noted:

$$\mathbf{A} = \mathbf{U}_{LA}\mathbf{\Lambda}_A\mathbf{U}_{RA}^T \tag{54}$$

Substituting Eq. (54) into (52) and simplifying yields:

$$\left\|\mathbf{r}_{q|Q}\right\|^2_{\mathbf{V}_q^{-1}} = \mathbf{z}_{Q*}^T\mathbf{U}_{RA}\mathbf{\Lambda}_A^2\mathbf{U}_{RA}^T\mathbf{z}_{Q*} \tag{55}$$

We use a second change of variable to recover a known quadratic form:

$$\mathbf{y}_A = \mathbf{U}_{RA}^T\mathbf{z}_{Q*} \quad , \quad \mathbf{y}_A \sim \mathrm{N}\left(\mathbf{U}_{RA}^T\mathbf{V}_Q^{-1/2}\mathbf{f}_Q \ , \ \mathbf{I}\right) \tag{56}$$

$$\left\|\mathbf{r}_{q|Q}\right\|^2_{\mathbf{V}_q^{-1}} = \mathbf{y}_A^T\mathbf{\Lambda}_A^2\ \mathbf{y}_A \tag{57}$$

which is equivalent to Eq. (23):

$$\left\|\mathbf{r}_{q|Q}\right\|^2_{\mathbf{V}_q^{-1}} = \sum_{i=1}^{p_{A,q}}\alpha_{A,i,q}^2 y_{A,i,q}^2$$

The coefficient $\alpha_{A,i,q}$ (subscript i ranging from 1 to $p_{A,q}$ at current time q) is the ith non-zero element of the diagonal matrix $\mathbf{\Lambda}_A$. The independent random variables $y_{A,i,q}$ are defined as:

$$y_{A,i,q} = \mathbf{T}_A^T \mathbf{y}_A$$

where the row vector $\mathbf{T}_A^T = \begin{bmatrix}\mathbf{0} & 1 & \mathbf{0}\end{bmatrix}$ is used to extract the ith element of $\mathbf{y}_A$. We have:

$$y_{A,i,q} \sim \mathrm{N}\left(\mathbf{T}_A^T \mathbf{U}_{RA}^T \mathbf{V}_Q^{-1/2} \mathbf{f}_Q \ , \ 1\right) .$$

This concludes the proof of Theorem I.

B. Proof Of Corollary to Theorem I: Distribution of Current-Time Test Statistic for Recursive Implementation

The corollary to Theorem I aims at expressing the probability distribution of $\left\|\mathbf{r}_{q|Q}\right\|^2_{\mathbf{V}_q^{-1}}$ without the batch matrices used in Eq. (24).

Equations (27) and (28) provide expressions of the current-time residual vector and covariance matrix:

$$\mathbf{r}_{q|Q} = \left(\mathbf{I} - \mathbf{H}_q \mathbf{K}_q\right)\mathbf{z}_q - \mathbf{H}_q\left(\mathbf{I} - \mathbf{K}_q \mathbf{H}_q\right)\hat{\mathbf{x}}_{q|Q-1}$$

$$\mathbf{R}_{q|Q} = \left(\mathbf{I} - \mathbf{H}_q \mathbf{K}_q\right)\mathbf{V}_q\left(\mathbf{I} - \mathbf{H}_q \mathbf{K}_q\right)^T - \mathbf{H}_q\left(\mathbf{I} - \mathbf{K}_q \mathbf{H}_q\right)\mathbf{P}_{q|Q-1}\left(\mathbf{I} - \mathbf{K}_q \mathbf{H}_q\right)^T \mathbf{H}_q^T$$

In general, $\mathbf{R}_{q|Q}$ is not invertible, which prevents direct derivation of the proof of the Corollary to Theorem I using a method akin to the proof of Theorem I.

Instead, we start the development by defining a matrix $\mathbf{B}$:

$$\mathbf{B} \equiv \mathbf{V}_q^{-1/2} \mathbf{R}_{q|Q}^{1/2} \tag{58}$$

The SVD of $\mathbf{B}$ is noted:

$$\mathbf{B} = \mathbf{U}_L \mathbf{\Lambda} \ \mathbf{U}_R^T \tag{59}$$

Matrix $\mathbf{\Lambda}$ is diagonal, with diagonal elements the singular values of the positive semi-definite matrix $\mathbf{B}$. Without loss of generality, we assume that the singular values of $\mathbf{B}$ are arranged in descending order on the diagonal of $\mathbf{\Lambda}$ (zero-valued singular values are grouped together on the diagonal of $\mathbf{\Lambda}$). Let $\mathbf{\Lambda}_{NZ}$ be the block matrix of $\mathbf{\Lambda}$ containing all non-zero singular values.

$$\mathbf{\Lambda}_{NZ} = \mathbf{T}_\Lambda \mathbf{\Lambda} \mathbf{T}_\Lambda^T$$

where $$\mathbf{T}_\Lambda = \begin{bmatrix}\mathbf{I} & \mathbf{0}\end{bmatrix}.$$

Matrix $\mathbf{\Lambda}$ can also be rewritten as $\mathbf{\Lambda} = \mathbf{T}_\Lambda^T \mathbf{\Lambda}_{NZ} \mathbf{T}_\Lambda$.

In addition, we define a vector $\mathbf{y}$ such that:

$$\mathbf{y} \equiv \mathbf{\Lambda}_{NZ}^{-1} \mathbf{T}_\Lambda \mathbf{U}_L^T \mathbf{V}_q^{-1/2} \mathbf{r}_{q|Q} \tag{60}$$

which yields:

$$\mathbf{V}_q^{-1/2} \mathbf{r}_{q|Q} = \mathbf{U}_L \mathbf{T}_\Lambda^T \mathbf{\Lambda}_{NZ} \mathbf{y} \tag{61}$$

Equation (61) is used to express the weighted norm of the residual as a quadratic form similar to Eq. (57). Equation (20) is rewritten as:

$$\left\|\mathbf{r}_{q|Q}\right\|_{\mathbf{V}_q^{-1}}^2 = \mathbf{r}_{q|Q}^T \mathbf{V}_q^{-1/2} \mathbf{V}_q^{-1/2} \mathbf{r}_{q|Q} \tag{62}$$

Substituting Eq. (61) into (62) yields:

$$\left\|\mathbf{r}_{q|Q}\right\|_{\mathbf{V}_q^{-1}}^2 = \mathbf{y}^T \mathbf{\Lambda}_{NZ}^2 \ \mathbf{y} \tag{63}$$

which is equivalent to Eq. (29):

$$\left\|\mathbf{r}_{q|Q}\right\|_{\mathbf{V}_q^{-1}}^2 = \sum_{i=1}^{p_q} \alpha_{i,q}^2 y_{i,q}^2 \, .$$

The coefficient $\alpha_{i,q}$ (subscript i ranging from 1 to p_q) is the ith element of the diagonal matrix $\mathbf{\Lambda}_{NZ}$. The normally distributed random variable $y_{i,q}$ is the ith element of vector $\mathbf{y}$. The covariance matrix of $\mathbf{y}$ is expressed by multiplying both sides of Eq. (60) by its transpose and by taking the expected value of the result:

$$\mathrm{E}\{\mathbf{y}\mathbf{y}^T\} = \mathbf{\Lambda}_{NZ}^{-1} \mathbf{T}_\Lambda \mathbf{U}_L^T \mathbf{V}_q^{-1/2} \mathbf{R}_{q|Q} \mathbf{V}_q^{-1/2} \mathbf{U}_L \mathbf{T}_\Lambda^T \mathbf{\Lambda}_{NZ}^{-1} \tag{64}$$

where $\mathrm{E}\{\}$ is the expected value operator. Then, we pre-multiply both sides of Eq. (64) by $\mathbf{U}_R \mathbf{\Lambda}^2 \mathbf{T}_\Lambda^T$ and post-multiply by $\mathbf{T}_\Lambda \mathbf{\Lambda}^2 \mathbf{U}_R^T$. We can simplify this expression using the fact that $\mathbf{\Lambda}^2 \mathbf{T}_\Lambda^T \mathbf{\Lambda}_{NZ}^{-1} \mathbf{T}_\Lambda = \mathbf{\Lambda}$, and by substituting Eq. (59) and (58) into the resulting expression. We obtain

$$\mathbf{U}_R \mathbf{\Lambda}^2 \mathbf{T}_\Lambda^T \mathrm{E}\{\mathbf{y}\mathbf{y}^T\} \mathbf{T}_\Lambda \mathbf{\Lambda}^2 \mathbf{U}_R^T = \mathbf{B}^T \mathbf{B} \mathbf{B}^T \mathbf{B} \tag{65}$$

In addition, because $\mathbf{U}_L^T \mathbf{U}_L = \mathbf{I}$ and substituting Eq. (59) for $\mathbf{U}_L \mathbf{\Lambda} \mathbf{U}_R^T$, Eq. (65) can be rewritten as:

$$\mathbf{B}^T \mathbf{U}_L \mathbf{\Lambda} \mathbf{T}_\Lambda^T \mathrm{E}\{\mathbf{y}\mathbf{y}^T\} \mathbf{T}_\Lambda \mathbf{\Lambda} \mathbf{U}_L^T \mathbf{B} = \mathbf{B}^T \mathbf{B} \mathbf{B}^T \mathbf{B}$$

The assertion that $\mathrm{E}\{\mathbf{y}\mathbf{y}^T\} = \mathbf{I}$ is equivalent to

$$\mathbf{B}^T \mathbf{U}_L \mathbf{\Lambda} \mathbf{\Lambda} \mathbf{U}_L^T \mathbf{B} = \mathbf{B}^T \mathbf{B} \mathbf{B}^T \mathbf{B}$$

which can be rewritten as:

$$\mathbf{B}^T \mathbf{U}_L \mathbf{\Lambda} \mathbf{U}_R^T \mathbf{U}_R \mathbf{\Lambda} \mathbf{U}_L^T \mathbf{B} = \mathbf{B}^T \mathbf{B} \mathbf{B}^T \mathbf{B} \, . \tag{66}$$

Substituting Eq. (59) into the left hand side of (66) shows that this expression is true. Therefore it must be true that

$$\mathrm{E}\{\mathbf{y}\mathbf{y}^T\} = \mathbf{I} \, . \tag{67}$$

Finally, Eq. (67) shows that the random variables $y_{i,q}$ in Eq. (29) are mutually independent for i ranging from 1 to p_q. Their probability distribution is given by:

$$y_{i,q} \sim \mathrm{N}\left(\begin{bmatrix}\mathbf{0} & \alpha_{i,q}^{-1} & \mathbf{0}\end{bmatrix}\mathbf{U}_L^T\mathbf{V}_q^{-1/2}\boldsymbol{\mu}_{R,q|Q}\ ,\ 1\right) \tag{68}$$

where $\boldsymbol{\mu}_{R,q|Q}$ is the mean vector of $\mathbf{r}_{q|Q}$. Vector $\boldsymbol{\mu}_{R,q|Q}$ can be written in terms of the current-time vector component $\mathbf{f}_q$ of $\mathbf{f}_Q$ and of the mean $\boldsymbol{\mu}_{q|Q}$ of $\hat{\mathbf{x}}_{q|Q}$ as:

$$\boldsymbol{\mu}_{R,q|Q} = \mathbf{f}_q - \mathbf{H}_q\boldsymbol{\mu}_{q|Q}\ .$$

This concludes the proof of the Corollary to Theorem I.

C. Proof of Theorem II: Statistical Independence between Current-Time State Estimates and Past-Time Residuals

For the purpose of this derivation, we consider the fault-free batch measurement equation:

$$\mathbf{z}_Q = \mathbf{H}_Q\mathbf{x}_Q + \mathbf{v}_Q \tag{69}$$

The fault vector $\mathbf{f}_Q$ in Eq. (3) is left aside because deterministic parts of the measurement error do not affect the determination of statistical independence. We refer to 'statistical independence' or 'stochastic independence' to designate independence of random parts of two or more vectors of variables.

As in Appendices I and II, we use a change of variable to normalize the measurement equation:

$$\mathbf{z}_{Q*} = \mathbf{H}_{Q*}\mathbf{x}_Q + \delta\mathbf{z}_Q \tag{70}$$

where:

$$\mathbf{z}_{Q*} = \mathbf{V}_Q^{-1/2}\mathbf{z}_Q \tag{71}$$

$$\mathbf{H}_{Q*} = \mathbf{V}_Q^{-1/2}\mathbf{H}_Q \quad \text{and} \quad \delta\mathbf{z}_Q = \mathbf{V}_Q^{-1/2}\mathbf{v}_Q$$

We have:

$$\delta\mathbf{z}_Q \sim \mathrm{N}(\mathbf{0}\ ,\ \mathbf{I}),$$

The state estimate and estimate error vectors can be expressed using the measurement Eq. (70) as:

$$\hat{\mathbf{x}}_{Q|Q} = \mathbf{S}_{Q*}\mathbf{z}_{Q*} \quad , \quad \delta\mathbf{x}_{Q|Q} = \mathbf{S}_{Q*}\delta\mathbf{z}_Q \tag{72}$$

where

$$\mathbf{S}_{Q*} = \left(\mathbf{H}_{Q*}^T\mathbf{H}_{Q*}\right)^{-1}\mathbf{H}_{Q*}^T \tag{73}$$

The measurement error vector $\delta\mathbf{z}_Q$ can be expressed as a sum of two orthogonal complements:

$$\delta\mathbf{z}_Q = \delta\mathbf{z}_{//,Q} + \delta\mathbf{z}_{\perp,Q}, \tag{74}$$

where $\delta\mathbf{z}_{//,Q}$ is the vector component of $\delta\mathbf{z}_Q$ that belongs to the column space of $\mathbf{H}_{Q*}$ (i.e., $\delta\mathbf{z}_{//,Q} \in \mathrm{Range}\left\{\mathbf{H}_{Q*}\right\}$) and $\delta\mathbf{z}_{\perp,Q}$ is the vector component of $\delta\mathbf{z}_Q$ belonging to the parity space of $\mathbf{H}_{Q*}$ (i.e., $\delta\mathbf{z}_{\perp,Q} \in \mathrm{Null}\left\{\mathbf{H}_{Q*}^T\right\}$).

In this two-part derivation, we first show that the current-time estimate error $\delta\mathbf{x}_{q|Q}$ is only a function of $\delta\mathbf{z}_{//,Q}$, and then we prove that $\delta\mathbf{z}_{//,Q}$ does not contribute to the past-time KF residual $\mathbf{r}_{k|K}$ (which is only a function of $\delta\mathbf{z}_{\perp,Q}$).

First, the current-time state estimate error can be expressed in terms of the batch vector:

$$\delta\mathbf{x}_{q|Q} = \begin{bmatrix}\mathbf{0} & \mathbf{I}\end{bmatrix}\delta\mathbf{x}_{Q|Q}\,. \tag{75}$$

Substituting Eq. (72) into (75) and using the definition of Eq. (74) yields:

$$\delta\mathbf{x}_{q|Q} = \begin{bmatrix}\mathbf{0} & \mathbf{I}\end{bmatrix}\mathbf{S}_{Q*}\left(\delta\mathbf{z}_{//,Q} + \delta\mathbf{z}_{\perp,Q}\right). \tag{76}$$

Considering the definition of $\mathbf{S}_{Q*}$ in Eq. (73), and because $\delta\mathbf{z}_{\perp,Q}$ is orthogonal to the columns of $\mathbf{H}_{Q*}$ the product $\mathbf{H}_{Q*}^T\delta\mathbf{z}_{\perp,Q}$ is zero. The result is then:

$$\delta\mathbf{x}_{q|Q} = \begin{bmatrix}\mathbf{0} & \mathbf{I}\end{bmatrix}\mathbf{S}_{Q*}\delta\mathbf{z}_{//,Q}\,. \tag{77}$$

The second part of the derivation aims at expressing past time KF residuals $\mathbf{r}_{k|K}$ (at discrete times k, for k ranging from 1 to q) as a function of batch measurement error vector components $\delta\mathbf{z}_{//,Q}$ and $\delta\mathbf{z}_{\perp,Q}$. The subset batch residual vector is expressed using Eq. (4) and (10) for the subset batch represented in Fig. 1 (there are no complications in the normalization step – indicated by '*' subscripts – because $\mathbf{V}_Q$ is block diagonal):

$$\mathbf{r}_{K|K} = \left(\mathbf{I} - \mathbf{H}_{K*}\mathbf{S}_{K*}\right)\mathbf{z}_{K*}\,. \tag{78}$$

The subset batch measurement equation (akin to Eq. (70)):

$$\mathbf{z}_{K*} = \mathbf{H}_{K*}\mathbf{x}_K + \delta\mathbf{z}_K$$

can be substituted into Eq. (78), which results in:

$$\mathbf{r}_{K|K} = \left(\mathbf{I} - \mathbf{H}_{K*}\mathbf{S}_{K*}\right)\delta\mathbf{z}_K\,. \tag{79}$$

because $\mathbf{S}_{K*}\mathbf{H}_{K*} = \mathbf{I}$. In addition, the relationship between subset and full batch measurement vectors is captured in the following equation:

$$\delta\mathbf{z}_K = \begin{bmatrix}\mathbf{I} & \mathbf{0}\end{bmatrix}\delta\mathbf{z}_Q \tag{80}$$

Substituting Eq. (80) into (79) and using the definition in (74) yields:

$$\mathbf{r}_{K|K} = \left(\mathbf{I} - \mathbf{H}_{K*}\mathbf{S}_{K*}\right)\begin{bmatrix}\mathbf{I} & \mathbf{0}\end{bmatrix}\left(\delta\mathbf{z}_{//,Q} + \delta\mathbf{z}_{\perp,Q}\right) \tag{81}$$

Next, we show that:

$$\left(\mathbf{I} - \mathbf{H}_{K*}\mathbf{S}_{K*}\right)\begin{bmatrix}\mathbf{I} & \mathbf{0}\end{bmatrix}\delta\mathbf{z}_{//,Q} = \mathbf{0} \tag{82}$$

Since $\delta\mathbf{z}_{//,Q}$ belongs to the range of $\mathbf{H}_{Q*}$, it can be expressed as:

$$\delta\mathbf{z}_{//,Q} = \mathbf{H}_{Q*}\mathbf{u}, \qquad \mathbf{u} \in \mathrm{R}^{m_Q} \tag{83}$$

where $\mathbf{u}$ is a $m_Q \times 1$ vector of real numbers. In addition, refer to Fig. 1 to see that $\mathbf{H}_{Q*}$ can be partitioned as:

$$\mathbf{H}_{Q*} = \begin{bmatrix}\mathbf{H}_{K*} & \mathbf{0} \\ \mathrm{X} & \mathrm{X}\end{bmatrix} \tag{84}$$

where 'X' indicates block matrices that are not directly relevant to this derivation. Substituting Eq. (84) into (83) and substituting the result into the left-hand-side of Eq. (82) yields:

$$\left(\mathbf{I}-\mathbf{H}_{K*}\mathbf{S}_{K*}\right)\begin{bmatrix}\mathbf{I} & \mathbf{0}\end{bmatrix}\begin{bmatrix}\mathbf{H}_{K*} & \mathbf{0}\\ \mathrm{X} & \mathrm{X}\end{bmatrix}\mathbf{u} \tag{85}$$

which simplifies to

$$\left(\mathbf{I}-\mathbf{H}_{K*}\mathbf{S}_{K*}\right)\begin{bmatrix}\mathbf{H}_{K*} & \mathbf{0}\end{bmatrix}\mathbf{u}\,. \tag{86}$$

Since it is true that

$$\mathbf{S}_{K*}\mathbf{H}_{K*}=\mathbf{I}\,, \tag{87}$$

then it must be true that Eq. (82) is satisfied. (As mentioned when deriving Eq. (78), the definition of $\mathbf{S}_{K*}$ is the same as $\mathbf{S}_{Q*}$ in Eq. (73) but applied to the normalized, subset batch equation).
Therefore, referring back to Eq. (81), we have established that:

$$\mathbf{r}_{K|K}=\left(\mathbf{I}-\mathbf{H}_{K*}\mathbf{S}_{K*}\right)\begin{bmatrix}\mathbf{I} & \mathbf{0}\end{bmatrix}\delta\mathbf{z}_{\perp,Q}$$

Similar to Eq. (21) for the full batch, the residual component at the last epoch of the subset batch residual is given by:

$$\mathbf{r}_{k|K}=\begin{bmatrix}\mathbf{0} & \mathbf{I}_{n_k}\end{bmatrix}\mathbf{r}_{K|K}=\begin{bmatrix}\mathbf{0} & \mathbf{I}_{n_k}\end{bmatrix}\left(\mathbf{I}_{n_K}-\mathbf{H}_{K*}\mathbf{S}_{K*}\right)\begin{bmatrix}\mathbf{I}_{n_K} & \mathbf{0}\end{bmatrix}\delta\mathbf{z}_{\perp,Q} \tag{88}$$

where subscripts of the identity matrices $\mathbf{I}$ indicate their dimensions. Finally, Eq. (77) and (88) prove that the current-time estimate error $\delta\mathbf{x}_{q|Q}$ and the past time KF residual vectors $\mathbf{r}_{k|K}$ (at any time *k,* for k ranging from 1 to q) are derived from orthogonal components of the full batch measurement error vector $\delta\mathbf{z}_Q$.

D. Proof of Theorem III: Mutual Independence between Current-Time and Past-Time Residuals

The residual $\mathbf{r}_{k|K}$ can be expressed in terms of the independent random vectors $\mathbf{z}_k$ and $\hat{\mathbf{x}}_{k|K-1}$:

$$\mathbf{r}_{k|K}=\left(\mathbf{I}-\mathbf{H}_k\mathbf{K}_k\right)\mathbf{z}_k-\mathbf{H}_k\left(\mathbf{I}-\mathbf{K}_k\mathbf{H}_k\right)\hat{\mathbf{x}}_{k|K-1}$$

Using the KF time-update equation ($\hat{\mathbf{x}}_{k|K-1}=\mathbf{\Phi}_{k-1}\hat{\mathbf{x}}_{k-1|K-1}$), we can also write that:

$$\mathbf{r}_{k|K}=\left(\mathbf{I}-\mathbf{H}_k\mathbf{K}_k\right)\mathbf{z}_k-\mathbf{H}_k\left(\mathbf{I}-\mathbf{K}_k\mathbf{H}_k\right)\mathbf{\Phi}_{k-1}\hat{\mathbf{x}}_{k-1|K-1} \tag{89}$$

In the next paragraph, we show that at any time *k*, the KF residuals $\mathbf{r}_{1|1}$ to $\mathbf{r}_{k-1|K-1}$ are all independent of $\mathbf{r}_{k|K}$, by showing that they are independent of both $\mathbf{z}_k$ and $\hat{\mathbf{x}}_{k-1|K-1}$ from which $\mathbf{r}_{k|K}$ is derived in Eq. (89).

First, the KF residual at any epoch k is computed using all previous measurements. Therefore, KF residuals $\mathbf{r}_{1|1}$ to $\mathbf{r}_{k-1|K-1}$ are all independent from $\mathbf{z}_k$ (they are computed using $\mathbf{z}_1$ to $\mathbf{z}_{k-1}$ only). Second, we apply Theorem II to the subset batch that uses measurements $\mathbf{z}_1$ to $\mathbf{z}_{k-1}$ (subscripts q and Q in Theorem II are replaced by $k-1$ and $K-1$). Theorem II states that $\hat{\mathbf{x}}_{k-1|K-1}$ is independent from residuals $\mathbf{r}_{1|1}$ to $\mathbf{r}_{k-1|K-1}$. Therefore, returning back to Eq. (89), the residual $\mathbf{r}_{k|K}$ is independent of all previous KF residuals from $\mathbf{r}_{1|1}$ to $\mathbf{r}_{k-1|K-1}$, and this is true at all times k, for k ranging between 1 and q.

Therefore, we have shown that the random parts of current and past-time KF residual components $\mathbf{r}_{k|K}$ are all mutually independent.

References

[1]Gertler, J., "A Survey of Model Based Failure Detection and Isolation in Complex Plants," *IEEE Control Systems Magazine*, Vol. 8, No.6, 1988, pp. 3-11.

[2]Wang, Y., Hussein, I., and Erwin, R., "Risk-Based Sensor Management for Integrated Detection and Estimation," *AIAA Journal of Guidance, Control, and Dynamics*, Vol. 34, No. 6, 2011, pp. 1767-1778.

[3]Velaga, N. R., Quddus, M. A., Bristow, A. L., and Zheng, Y., "Map-Aided Integrity Monitoring of a Land Vehicle Navigation System," *IEEE Transactions on Intelligent Transportation Systems*, Vol. 13, No. 2, 2012, pp. 848-858.

[4]RTCA Special Committee 159, "Minimum Operational Performance Standards for Global Positioning System/Wide Area Augmentation System Airborne Equipment," RTCA/DO-229C, 2001.

[5]RTCA Special Committee 159, "Minimum Aviation System Performance Standards for the Local Area Augmentation System (LAAS)," RTCA/DO-245, 2004.

[6]Blanch, J., Ene, A., Walter, T., and Enge, P., "An Optimized Multiple Hypothesis RAIM Algorithm for Vertical Guidance," *Proceedings of the 20th International Technical Meeting of the Satellite Division of The Institute of Navigation (ION GNSS 2007)*, Fort Worth, TX, 2007, pp. 2924-2933.

[7]Lee, Y. C., "Analysis of Range and Position Comparison Methods as a Means to Provide GPS Integrity in the User Receiver," *Proceedings of the 42nd Annual Meeting of The Institute of Navigation*, Seattle, WA, 1986, pp. 1-4.

[8]Parkinson, B. W., and Axelrad, P., "Autonomous GPS Integrity Monitoring Using the Pseudorange Residual," *NAVIGATION: Journal of the Institute of Navigation*, Vol. 35, No. 2, 1988, pp. 225-274.

[9]Brown, R., "Receiver Autonomous Integrity Monitoring," *Global Positioning System: Theory and Applications Volume 2*, edited by Parkinson, B. W., and Spilker, J. J. Jr., Progress in Astronautics and Aeronautics, AIAA, Washington, DC, Vol. 163, 1996, pp. 143-166.

[10]Willsky, A., "A survey of design methods for failure detection in dynamic systems," *Automatica*, Vol. 12, 1976, pp. 601-611.

[11]Sobel, M., and Wald, A., "A Sequential Decision Procedure for Choosing One of Three Hypotheses Concerning the Unknown Mean of a Normal Distribution," *The Annals of Mathematical Statistics*, Vol. 20, No. 4, 1949, pp. 502-522.

[12]Page, E. S., "Continuous inspection schemes," *Biometrika*, Vol. 41, 1954, pp. 100-115.

[13]Lorden, G., "Procedures for reacting to a change in distribution," *The Annals of Mathematical Statistics*, Vol. 42, No. 6, 1971, pp. 1897-1908.

[14]Shiryayev, A. N., *Optimal Stopping Rules*, Springer-Verlag, New York, 1978.

[15]Malladi, D. P., and Speyer, J. L., "A Generalized Shiryayev Sequential Probability Ratio Test for Change Detection and Isolation," *IEEE Transactions on Automatic Control*, Vol. 44, No. 8, 1999, pp. 1522-1534.

[16]Brown, R. G. and Hwang, Y. C., "GPS failure detection by autonomous means within the cockpit," *Proceedings of the 42nd Annual Meeting of the Institute of Navigation*, Seattle, WA, 1986, pp. 5-12.

[17]White, N. A., Maybeck, P. S., and DeVilbiss, S. L, "Detection of Interference/Jamming and Spoofing in a DGPS-Aided Inertial System," *IEEE Transactions on Aerospace and Electronic Systems*, Vol. 34, No. 4, Oct. 1998, pp. 1208-1217.

[18]Chan, S., and Speyer, J. L., "A Sequential Probability Test for RAIM," *Proceedings of the 17th International Technical Meeting of the Satellite Division of The Institute of Navigation (ION GNSS 2004)*, Long Beach, CA, 2004, pp. 1798-1802.

[19]Willsky, A., and Jones, H., "A generalized likelihood ratio approach to the detection and estimation of jumps in linear systems," *IEEE Transactions on Automatic Control*, Vol. 21, No. 1, Feb. 1976, pp. 108 – 112.

[20]Chow, E., and Willsky, A., "Analytical redundancy and the design of robust failure detection systems," *IEEE Transactions on Automatic Control*, Vol. 29 , No. 7, 1984, pp. 603-614.

[21]Sukkarieh, S., Nebot, E. M., and Durrant-Whyte, H.F., "A High Integrity IMU/GPS Navigation Loop for Autonomous Land Vehicle Applications," *IEEE Transactions on Robotics and Automation*, Vol. 15, No. 3, Jun. 1999, pp. 572–578.

[22]Abuhashim, T. S., Abdel-Hafez, M. F., and Al-Jarrah, M.-A., "Building a Robust Integrity Monitoring Algorithm for a Low Cost GPS-aided-INS System," *International Journal of Control, Automation, and Systems*, Vol. 8, No. 5, 2010, pp.1108-1122.

[23]Friséna, M., "Optimal Sequential Surveillance for Finance, Public Health, and Other Areas," *Sequential Analysis: Design Methods and Applications*, Vol. 28, No. 3, 2009, pp. 310-337.

[24]Lai, T. L., "Sequential Multiple Hypothesis Testing and Efficient Fault Detection-Isolation in Stochastic Systems," *IEEE Transactions on Information Theory*, Vol. 46, No. 2, 2000, pp. 595-608.

[25]Sullivan, E. J., and Candy, J. V., "Sequential Detection Estimation and Noise Cancellation," *Imaging for Detection and Identification, NATO Security through Science Series*, 2007, pp 97-105.

[26]Dionne, D., Oshman, Y., and Shinar, D., "Novel Adaptive Generalized Likelihood Ratio Detector with Application to Maneuvering Target Tracking," *AIAA Journal of Guidance, Control, and Dynamics*, Vol. 29, No. 2, 2006, pp. 465-474.

[27]Hewitson, S., and Wang, J., "Extended Receiver Autonomous Integrity Monitoring (eRAIM) for GNSS/INS Integration," *Journal of Surveying Engineering*, Vol. 136, No. 1, Feb. 2010, pp. 13-22.

[28]Diesel, J., and Luu, S., "GPS/IRS AIME: Calculation of Thresholds and Protection Radius Using Chi-Square Methods," *Proceedings of the 8th International Technical Meeting of the Satellite Division of The Institute of Navigation (ION GPS 1995)*, Palm Springs, CA, 1995, pp. 1959-1964.

[29]Nikiforov, I., "New optimal approach to Global Positioning System/Differential Global Positioning System integrity monitoring," *AIAA Journal of Guidance, Control, and Dynamics*, Vol.19, No.5, 1996, pp. 1023-1033.

[30]Bakhache, B., "A Sequential RAIM Based on the Civil Aviation Requirements,' *Proceedings of the 12th International Technical Meeting of the Satellite Division of The Institute of Navigation (ION GPS 1999)*, Nashville, TN, 1999, pp. 1201-1210.

[31]Clot, A., Macabiau, C., Nikiforov, I., and Roturier, B., "Sequential RAIM Designed to Detect Combined Step Ramp Pseudo-Range Error," *Proceedings of the 19th International Technical Meeting of the Satellite Division of The Institute of Navigation (ION GNSS 2006)*, Fort Worth, TX, 2006, pp. 2621-2633.

[32]Brenner, M., "lntegrated GPS/lnertial Fault Detection Availability," *Proceedings of the 8th International Technical Meeting of the Satellite Division of The Institute of Navigation (ION GPS 1995)*, Palm Springs, CA, 1995, pp. 1949-1958.

[33]Joerger, M., Gratton, L., Pervan, B., and Cohen, C. E., "Analysis of Iridium-Augmented GPS for Floating Carrier Phase Positioning," *NAVIGATION: Journal of the Institute of Navigation*, Vol. 57, No. 2, Summer 2010, pp. 137-160.

[34]Bryson, A. E., *Applied Linear Optimal Control*, Cambridge University Press, Cambridge, England, UK, 2002, pp. 310-312.

[35]Sturza, M., "Navigation System Integrity Monitoring Using Redundant Measurements," *NAVIGATION: Journal of the Institute of Navigation*, Vol. 35, No. 4, 1988, pp. 69-87.

[36]Pervan, B., "Navigation integrity for aircraft precision landing using the global positioning system," Ph.D. Dissertation, Stanford University, Aeronautics and Astronautics Dept., Stanford, CA, 1996.

[37]Joerger, M., and Pervan, B., "Sequential Residual-Based RAIM," *Proceedings of the 23rd International Technical Meeting of The Satellite Division of the Institute of Navigation (ION GNSS 2010)*, Portland, OR, 2010, pp. 3167-3180.

[38]Ropokis, G., Rontogiannis, A., and Mathiopoulos, P., "Quadratic forms in normal RVs: Theory and applications to OSTBC over Hoyt fading channels," *IEEE Transactions on Wireless Communications*, Vol. 7, No. 12, 2008, pp.5009 - 5019.

[39]Davies, R. B., "Algorithm AS 155: The Distribution of a Linear Combination of $\chi 2$ Random Variables," *Journal of the Royal Statistical Society, Series C (Applied Statistics)*, Vol. 29, No. 3, 1980, pp. 323-333.

[40]Joerger, M., Neale, J., and Pervan, B., "Iridium/GPS Carrier Phase Positioning and Fault Detection Over Wide Areas," *Proceedings of the 22nd International Technical Meeting of The Satellite Division of the Institute of Navigation (ION GNSS 2009)*, Savannah, GA, 2009, pp. 1371-1385.

[41]Angus, J. E., "RAIM with multiple faults," *NAVIGATION: Journal of the Institute of Navigation*, Vol. 53, No. 4, 2007, pp.249-257.

[42]Parkinson, B., and J. Spilker, *Global Positioning System: Theory and Applications Volume 1*, AIAA Progress in Aeronautics and Astronautics, Washington, DC, Vol. 163, 1996.

[43]McGraw, G., Murphy, T., Brenner, M., Pullen, S., and Van Dierendonck, A., "Development of the LAAS Accuracy Models," *Proceedings of the Institute of Navigation GPS Conference*, Salt Lake City, UT, 2000, pp. 1212-1223.